



## Obrabotka metallov -

## Metal Working and Material Science

Journal homepage: [http://journals.nstu.ru/obrabotka\\_metallov](http://journals.nstu.ru/obrabotka_metallov)



### Evaluation of vacancy formation energy for BCC-, FCC-, and HCP-metals using density functional theory

Yulia Emurlaeva<sup>1, a,\*</sup>, Daria Lazurenko<sup>1, b</sup>, Zinaida Bataeva<sup>2, c</sup>, Ivan Petrov<sup>3, d</sup>, Gleb Dovzhenko<sup>4, e</sup>,  
 Lubov Makogon<sup>2, f</sup>, Maksim Khomyakov<sup>5, g</sup>, Kemal Emurlaev<sup>1, h</sup>, Ivan Bataev<sup>1, i</sup>

<sup>1</sup> Novosibirsk State Technical University, 20 Prospekt K. Marksa, Novosibirsk, 630073, Russian Federation

<sup>2</sup> Siberian State University of water transport, 33 Schetinkina str., Novosibirsk, 630099, Russian Federation

<sup>3</sup> Novosibirsk State University, 1 Pirogova str., Novosibirsk, 630090, Russian Federation

<sup>4</sup> Siberian Circular Photon Source “SKIF” Borekov Institute of Catalysis of Siberian Branch of the Russian Academy of Sciences (SRF “SKIF”), 1 Nikol’skii pr., Kol’tsovo, 630559, Russian Federation

<sup>5</sup> Institute of Laser Physics of Siberian Branch of the Russian Academy of Sciences, 15B Prospekt Ak. Lavrentieva, Novosibirsk, 630090, Russian Federation

<sup>a</sup> <https://orcid.org/0000-0003-4835-4134>, [emurlaeva@corp.nstu.ru](mailto:emurlaeva@corp.nstu.ru), <sup>b</sup> <https://orcid.org/0000-0002-2866-5237>, [pavlyukova\\_87@mail.ru](mailto:pavlyukova_87@mail.ru),

<sup>c</sup> <https://orcid.org/0000-0001-5027-6193>, [bataevazb@ngs.ru](mailto:bataevazb@ngs.ru), <sup>d</sup> <https://orcid.org/0000-0002-7968-1130>, [ivan77766600@outlook.com](mailto:ivan77766600@outlook.com),

<sup>e</sup> <https://orcid.org/0000-0003-0615-0643>, [g.dovzhenko@skif.ru](mailto:g.dovzhenko@skif.ru), <sup>f</sup> <https://orcid.org/0009-0006-1463-0697>, [ledimakogon@mail.ru](mailto:ledimakogon@mail.ru),

<sup>g</sup> <https://orcid.org/0000-0001-8095-2092>, [mnkhomy@gmail.com](mailto:mnkhomiy@gmail.com), <sup>h</sup> <https://orcid.org/0000-0002-1114-6799>, [emurlaev@corp.nstu.ru](mailto:emurlaev@corp.nstu.ru),

<sup>i</sup> <https://orcid.org/0000-0003-2871-0269>, [i.bataev@corp.nstu.ru](mailto:i.bataev@corp.nstu.ru)

#### ARTICLE INFO

##### Article history:

Received: 10 April 2023

Revised: 18 April 2023

Accepted: 27 April 2023

Available online: 15 June 2023

##### Keywords:

Metals

Vacancy formation energy

Diffusion

Simulation

Density functional theory

##### Funding

This study was funded by the Federal Task of Ministry of Education and Science of the Russian Federation (project FSUN-2020-0014 (2019-0931): “Investigations of Metastable Structures Formed on Material Surfaces and Interfaces under Extreme External Impacts”).

##### Acknowledgements:

Researches were conducted at core facility of NSTU “Structure, mechanical and physical properties of materials”.

**For citation:** Emurlaeva Yu.Yu., Lazurenko D.V., Bataeva Z.B., Petrov I.Yu., Dovzhenko G.D., Makogon L.D., Khomyakov M.N., Emurlaev K.I., Bataev I.A. Evaluation of vacancy formation energy for BCC-, FCC-, and HCP-metals using density functional theory. *Obrabotka metallov (tehnologiya, oborudovanie, instrumenty) = Metal Working and Material Science*, 2023, vol. 25, no. 2, pp. 104–116. DOI: 10.17212/1994-6309-2023-25.2-104-116. (In Russian).

##### \* Corresponding author

Emurlaeva Yu. Yu., Assistant

Novosibirsk State Technical University,

20 Prospekt K. Marksa,

630073, Novosibirsk, Russian Federation

Tel.: 8 (383) 346-06-12, e-mail: [emurlaeva@corp.nstu.ru](mailto:emurlaeva@corp.nstu.ru)

#### ABSTRACT

**Introduction.** Vacancies are among the crystal lattice defects that have a significant effect on the structural transformations processes during thermal, chemical-thermal, thermomechanical, and other types of alloys treatment. The vacancy formation energy is one of the most important parameters used to describe diffusion processes. An effective approach to its definition is based on the use of the *density functional theory (DFT)*. The main advantage of this method is to carry out computations without any parameters defined empirically. **The purpose of the work** is to estimate vacancy formation energy of BCC-, FCC- and HCP-metals widely used in mechanical engineering and to compare these findings obtained using various exchange-correlation functionals (*GGA* and *meta-GGA*). **Computation procedure.** The computations were carried out using the projector-augmented wave method using the *GPAW* code and the atomic simulation environment (*ASE*). The *Perdew-Burke-Ernzerhof*, *MGGAC* and *rMGGAC* functionals were used. The wave functions were described by plane waves within simulations. Vacancies formation energy was evaluated using supercells approach with a size  $3 \times 3 \times 3$ . Computations were carried out for BCC-metals (*Li, Na, K, V, Cr, Fe, Rb, Nb, Mo, Cs, Ta, W*), FCC-metals (*Al, Ni, Cu, Rh, Pd, Ag, Ir, Pt, Au, Pb, Co*) and HCP-metals (*Be, Ti, Zr, Mg, Sc, Zn, Y, Ru, Cd, Hf, Os, Co, Re*). **Results and discussion.** A comparison of the defined vacancy formation energies indicates the validity of the following ratio of values:  $E_f^{PBE} < E_f^{MGGAC} \leq E_f^{rMGGAC}$ . The values

obtained using the open source *GPAW* code are characterized by the same patterns as for widely spread commercially distributed program *VASP*. It was revealed that the use of the *PBE* and *MGGAC* functionals leads to a slight deviation relative to the experimentally determined vacancies formation energy in contrast to the computations using *rMGGAC*.



## Introduction

Point defects, particularly vacancies, determine considerably the nature of various phenomena that occur in metals and alloys. The presence of vacancies is one of the most critical factors that is taken into consideration in the qualitative and quantitative description of diffusion processes accompanying thermal and thermochemical treatment of metals. For instance, recrystallization that develops in plastically deformed materials is based on the phenomenon of self-diffusion, which is closely related to the characteristics of vacancy migration [1, 2]. Polygonization in deformed metals is closely associated with a climb of edge dislocations which is accompanied by the emission or absorption of vacancies [1, 2].

Vacancies have a significant effect on the kinetics of diffusive phase transformations. The coagulation of multiple vacancies is considered as one of the main reasons for the formation of the so-called *Kirkendall* porosity observed during diffusion welding of some alloys [3–6]. Interstitial defects and vacancies are also essential underway irradiation-induced swelling that is one of the major tasks in nuclear engineering.

The key parameter to describe vacancies is the energy of its formation. There are a number of experimental methods to evaluate the vacancy formation energy (*VFE*) to date. Methods based on precision measurement of heat capacity, electrical resistivity analysis, and positron annihilation spectroscopy (*PAS*) are among it [7–9]. It should be noted that the experimental determination of the formation energy of point defects is an extremely time-consuming process and is characterized by insufficient accuracy.

The appearance and development of effective computational methods, among which the density-functional theory (*DFT*) should especially emphasized, is the result of the intensive development of computational materials science methods used, among other things, for the analysis of defects in the crystal structure. Using *DFT*, one can easily evaluate the ground state energy for any substance [10] without the introduction of some sort of empirically determined parameters for the calculations. Thus, point defect formation energy can be defined as the difference between the energy values of a supercell containing a vacancy (vacancy supercell,  $E_{tot}^{vac}$ ) and a defect-free supercell (bulk supercell,  $E_{tot}^{bulk}$ ). The value obtained by the *DFT* requires a number of additional corrections to compare with the empirically determined parameters. The features of this approach are described in detail in review publications [11, 12].

One of the stages of *DFT* computation is associated with the choice of the exchange-correlation (*XC*) functional. The exact shape of functionals is currently unknown [13] therefore its approximations are used in practice. It should be noted that even if the chosen approximation of *XC* functional gives the correct result in evaluating some physical property, it may not be appropriate for evaluating another one. There are two widespread approximations among the great number of possible models of *XC* functionals, namely: the local density approximation (*LDA*) based on the free electron model [13, 14] and the generalized gradient approximation (*GGA*) that takes into account not only the electron density, but also its gradient at the considered point in space [15]. Both *LDA* and *GGA* functionals are based on a number of simplifications and, for this reason, are characterized by a certain inaccuracy. The choice of a particular *XC* functional depends on the type of task being solved. For instance, the cohesive energy using *GGA*-model can be defined more precisely [16] and therefore *GGA* can be effectively used to calculate the point defects formation energy including vacancies (*VFE*). However, the inaccuracy of the *VFE* using the *GGA* functional turned out to be quite high in practice [17]. In the review paper [11], *Freysoldt et al.* highlight that using of *LDA* functional provides a higher accuracy of the *VFE* evaluating in comparison with computation using *GGA*. It is associated with the assessment of the inner surface energy contribution arising when one of the atoms is removed from the supercell.

The development of new *XC* functionals and its application for the calculation of various characteristics of materials, including the *VFE*, make it possible to minimize the deviation of the calculated data from the experimental ones. In particular, the paper [18] reports about efficiency of meta-*GGA*-functionals. Meta-*GGA* functionals contain the second derivative of the electron density and also take into account the kinetic-energy density of electrons, and therefore provide better precision. However, the computations of *VFE* via the *revTPSS* functional (one of the most commonly used meta-*GGA* functionals) did not confirm this

hypothesis [8]. Thus, the search for  $XC$  functionals that make it possible to improve the accuracy of  $VFE$  calculations for metals remains an urgent task.

The aim of this work was to evaluate the  $VFE$  of  $BCC$ -,  $FCC$ - and  $HCP$ -metals widely used in mechanical engineering using  $DFT$  and to compare the results obtained by application of various types of  $XC$  functionals ( $GGA$  and meta- $GGA$ ). The results obtained are important for analyzing the effectiveness of  $DFT$  computations of point defect formation energy. In addition, the obtained data can be used for reference purposes in the simulation of diffusion processes.

### Theoretical background

The calculations were carried out using the projector-augmented wave ( $PAW$ ) method with the application of the  $GPAW$  code [19, 20] and the atomic simulation environment ( $ASE$ ) [21], implemented in the Python programming language. The widely used *Perdew-Burke-Ernzerhof* ( $PBE$ ) functional of  $GGA$  family [22], as well as  $MGGAC$  [23] and  $rMGGAC$  [24] functionals were used to describe  $XC$  potential. The  $MGGAC$  functional proposed in [23] is developed for quantum chemistry computations and solid state physics. The authors of this model combined the resulting meta- $GGA$  exchange functional with the  $GGA$  correlation one. Using this combination, one can determine the structural and energy properties of solids with high accuracy. The  $rMGGAC$  functional proposed by *Jana et al.* [24] accounts for mismatches in the correlation energy of  $MGGAC$  for atoms and ions.

The wave functions were described with plane waves. The cut-off energy of 500 eV was used for the plane-wave basis set. Total numbers of  $k$ -points generated according to *Monkhorst-Pack* method was 27 ( $3 \times 3 \times 3$  along the  $X$ ,  $Y$  and  $Z$  axes) for the chosen functionals ( $PBE$ ,  $MGGAC$  and  $rMGGAC$ ). To improve convergence with respect to *Brillouin* zone sampling, *Marzari-Vanderbilt* distribution (cold smearing) with the temperature broadening parameter of 0.2 eV was applied [25]. The energy of vacancy formation was evaluated using supercells approach with a size of  $3 \times 3 \times 3$ . Detailed information about the parameters used in the computations is given in **Appendix A**.

Calculations were carried out for the following metals:

- 1)  $BCC$ -metals: *Li, Na, K, V, Cr, Fe, Rb, Nb, Mo, Cs, Ta, W*.
- 2)  $FCC$ -metals: *Al, Ni, Cu, Rh, Pd, Ag, Ir, Pt, Au, Pb, Co*.
- 3)  $HCP$ -metals: *Be, Ti, Zr, Mg, Sc, Zn, Y, Ru, Cd, Hf, Os, Co, Re*.

To calculate the formation energy of point defect  $X$  via  $DFT$ , one can use the following formula [11]:

$$E^f[X^q] = E_{tot}[X^q] - E_{tot}[bulk] - \sum_i n_i \mu_i + qE_F + E_{corr}, \quad (1)$$

where  $E^f[X^q]$  is the energy of defect  $X$  in charge state  $q$ ;  $E_{tot}[X^q]$  is the total energy of a supercell containing the defect;  $E_{tot}[bulk]$  is the total energy of the perfect supercell;  $n_i$  is a number of atoms of type  $i$  that have been added to (in this case it is assumed that  $n_i > 0$ ) or removed from (in this case it is assumed that  $n_i < 0$ ) the supercell to form the defect;  $\mu_i$  are the corresponding chemical potentials of the added or removed atoms;  $E^f$  is the Fermi energy and  $E_{corr}$  is a correction term that accounts for finite  $k$ -point sampling in the case of shallow impurities (a common term used in the physics of semiconductor).

In the case of single vacancy (or monovacancy) formed in a pure metal  $q = 0$ ;  $E_{corr} = 0$ ;  $i = 1$ ;  $n_1 = n = -1$ . Thus, the equation (1) is significantly simplified and takes the following form:

$$E^f[vac] = E_{tot}[vac] - E_{tot}[bulk] + \mu, \quad (2)$$

where  $\mu$  is the chemical potential of the metal analyzed (the chemical potential of a single-element compound is typically used in  $DFT$  calculations [26]).

This means that the  $VFE$  can be derived as the energy difference between a supercell that contains a vacancy and a perfect one (defect-free supercell). However, the total energy is an extensive quantity. In

other words, the energy of the system increases proportionally to the number of atoms contained therein. A supercell containing a monovacancy obviously has one atom less than a perfect one. Thus, its energy (excluding the vacancy effect) will be lower compared to the energy of a perfect supercell. Therefore, to distinguish the vacancy contribution one needs to add the chemical potential of the removed atom to the resulting energy difference according to the equation (2). It should be noted that the issue of point defect energy formation definition is more complex for semiconductors and ionic crystals in contrast to metals [11].

## Results and Discussion

It is known, that the *VFE* in metals is well described through the following relationship:

$$E_f \approx AkT_m, \quad (3)$$

where  $T_m$  is a melting temperature (K);  $k$  is the Boltzmann constant;  $A$  is a proportionality constant close to 10 [27].

*Hayashiuchi et al.* believed that a relationship between the *VFE* and the melting point is caused by the similarity between processes of atomic movement during vacancy formation and also its movement at the “solid – liquid” boundary during melting. According to this theory  $A \approx 9.7$ .

Fig. 1 shows the research findings in the coordinates “ $E_f - T_m$ ”. It can be noted that the trend of *ViFE* growth with the melting temperature of the material is confirmed by data obtained using various methods. The trends defined in this work have a similar character with the *DFT* computations carried out by *Medasani et al.* using the *VASP* computer program [8]. This fact testifies about the appropriateness of using of open source *GPW* code as to alternative to widely used commercial software package *VASP*. The computational results carried out within this work and those obtained by other authors (including the experimental findings) are summarized in **Appendix B**.

The proportionality constant  $A$ , evaluated based on the results obtained using *PAS*, is close to  $\sim 12.1$ . It is slightly above the  $A = 10$  proposed in [27–29]. The proportionality constant was found to be approxi-

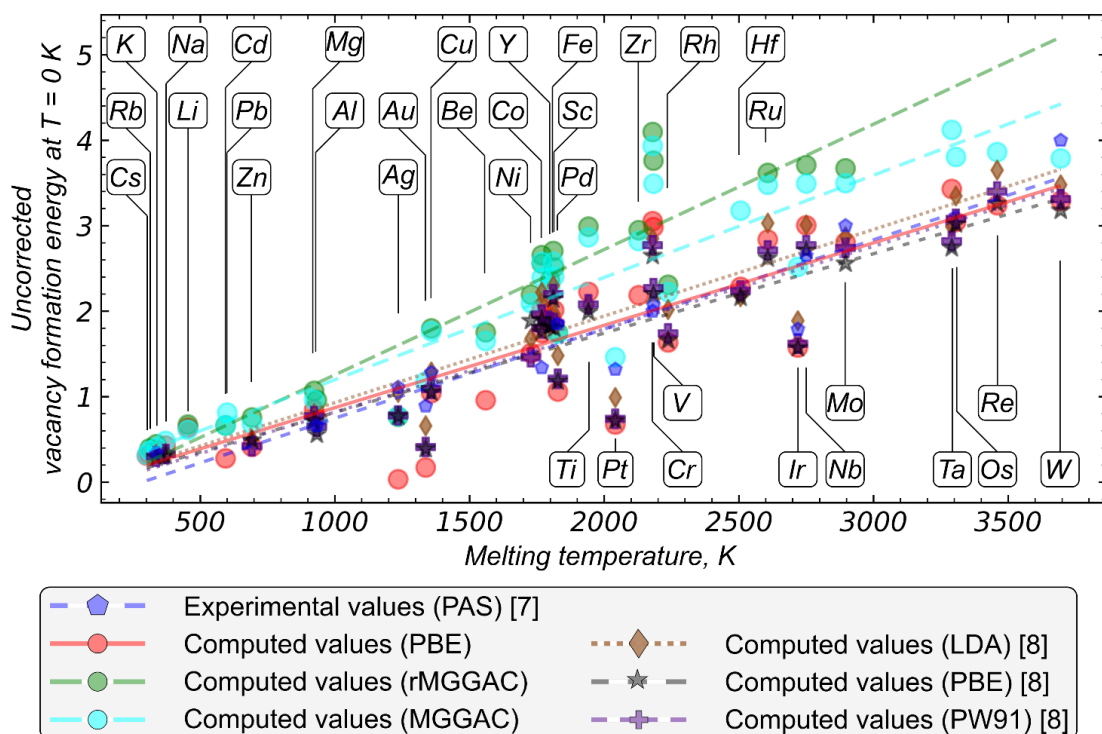


Fig. 1. Vacancy formation energy in various metals according to its melting point

mately equal to  $\sim 11.6$ ,  $\sim 13.9$  and  $\sim 17.0$  within the computation of  $VFE$  using  $PBE$ ,  $MGGAC$  and  $rMGGAC$  respectively. Thus, the results obtained using the widespread  $PBE$  XC functional are considerably closer to the experimental data.

The scatter in the computed results relative to the experimental data can be evaluated using mean square error ( $MSE$ ). In this paper, it was calculated according to the following equation:

$$MSE = \frac{\sum (E_f^{calc_i} - E_f^{exp_i})^2}{n}, \quad (4)$$

where  $E_f^{calc_i}$  and  $E_f^{exp_i}$  are the calculated and experimental  $VFE$  for element of type  $i$ , respectively.

It should be noted that only experimental values of the  $VFE$ , measured using  $PAS$  [7], were used in this study. Since the experimental data are presented only for some metals [7], the deviation of the calculated energies remained unknown for the rest, and, for this reason, was not taken into account to calculate the  $MSE$ .

The  $MSEs$  are close for  $PBE$  and  $MGGAC$  functionals ( $0.66$  and  $0.64 \text{ eV}^2$ , respectively). When using  $rMGGAC$ , the  $MSE$  is significantly higher ( $1.11 \text{ eV}^2$ ).

Using fig. 2, one can compare the  $VFE$  calculated within this study with the experimental results. The comparison of findings was carried out according to the approach proposed by *Medasani et al.* [8]. From the calculated data, it is clear that the use of the  $rMGGAC$  and  $MGGAC$  functionals results in  $VFE$  overestimation as compared to the experimental values. The  $VFE$  computed using the widespread  $PBE$  functional quite uniformly distributed relative to the  $y = x$  line. In general, the results obtained are characterized by the following trend:  $E_f^{PBE} < E_f^{MGGAC} \leq E_f^{rMGGAC}$  that is well correlated with the findings of *Medasani et al.* [8].

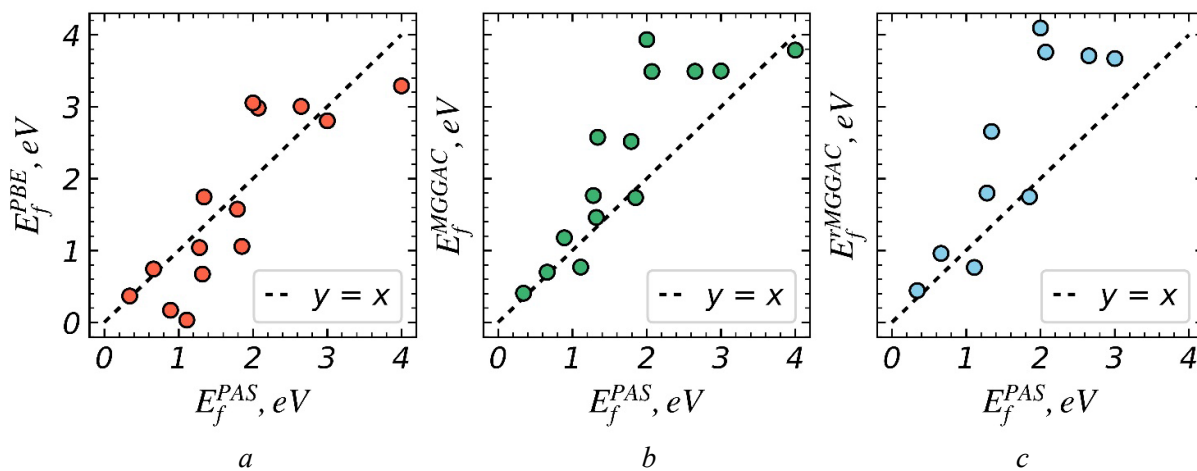


Fig. 2. Comparison of experimental and computed values of the vacancy formation energy for the exchange-correlation functionals  $PBE$  (a),  $rMGGAC$  (b) and  $MGGAC$  (c). The dotted line representing the function  $y = x$  is shown on the graphs for the convenience of analyzing the obtained data

Analyzing the obtained results, it can be noted that patterns defined by computing correspond to the experimental data. The typical dependence of the  $VFE$  from the melting temperature was mentioned above. Nevertheless, it is difficult to use the  $VFE$  estimated using  $DFT$  in subsequent calculations without introducing additional corrections. In particular, the equilibrium concentration of vacancies and the diffusion coefficient depend exponentially on the  $VFE$ . It means that these parameters extremely sensitive to the error in determining the latter one. According to *T. Mattsson* and *A. Mattsson* [30], to obtain a reasonable value of the defects' equilibrium concentration at room temperature one need to know the  $VFE$  with an accuracy of  $0.025 \text{ eV}$ . From the presented data it follows that this accuracy is unreachable without additional corrections. One of the approaches used for a posteriori correction of the  $VFE$  is to account the energy of the inner surface inside the crystal created by removing one of the atoms [30].

## Conclusions

The analysis of *VFE* in *BCC*-, *FCC*- and *HCP*-metals was carried out using *DFT* simulation. Based on the conducted study, the following conclusions can be made.

1. The use of *DFT* is an effective approach to evaluate the formation energy of point defects. The *VFE* obtained via open source *GPW* code are characterized by the same trends as the widely spread commercial software package *VASP*. It is reasonable to compare the application efficiency of both programs in terms of calculation accuracy and rate in further studies.

2. In most cases, the use of the *PBE* and *MGGAC* functionals provides a slighter deviation relative to the experimentally defined *VFE* in comparison with the calculation via *rMGGAC*.

3. A comparison of the computed *VFE* indicates the validity of the following ratio:  $E_f^{PBE} < E_f^{MGGAC} \leq E_f^{rMGGAC}$ .

4. Despite common patterns, the calculated *VFE* may differ significantly from the experimental data. Thus, the *VFE* evaluated at  $T = 0$  K can be used only in comparative studies. To increase the accuracy, the calculated *VFE* should be subject to additional correction.

## References

1. Gorelik S.S., Dobatkin S.V., Kaputkina L.M. *Rekristallizatsiya metallov i splavov* [Recrystallization of metals and alloys]. Moscow, MISiS Publ., 2005. 432 p. ISBN: 5-87623-103-7.
2. Humphreys F.J., Hatherly M. *Hatherly recrystallization and related annealing phenomena*. 2nd ed. Elsevier, 2004. 605 p. DOI: 10.1016/B978-0-08-044164-1.X5000-2.
3. Siegel R.W. Vacancy concentrations in metals. *Journal of Nuclear Materials*, 1978, vol. 69–70, pp. 117–146. DOI: 10.1016/0022-3115(78)90240-4.
4. Mehrer H. *Diffusion in solids: fundamentals, methods, materials, diffusion-controlled processes*. Springer, 2007. 673 p. DOI: 10.1007/978-3-540-71488-0.
5. Smigelskas A.D., Kirkendall E.O. Zinc diffusion in alpha brass. *Transactions of AIME*, 1947, vol. 171, pp. 130–142.
6. Paul A., Laurila T., Vuorinen V., Divinski S. *Thermodynamics, diffusion and the Kirkendall effect in solids*. Springer, 2014. 530 p. DOI: 10.1007/978-3-319-07461-0.
7. Kraftmakher Y. Equilibrium vacancies and thermophysical properties of metals. *Physics Reports*, 1998, vol. 299, iss. 2–3, pp. 79–188. DOI: 10.1016/s0370-1573(97)00082-3.
8. Medasani B., Haranczyk M., Canning A., Asta M. Vacancy formation energies in metals: A comparison of MetaGGA with LDA and GGA exchange–correlation functionals. *Computational Materials Science*, 2015, vol. 101, pp. 96–107. DOI: 10.1016/j.commatsci.2015.01.018.
9. Gong Y., Grabowski B., Glensk A., Körmann F., Neugebauer J., Reed R.C. Temperature dependence of the Gibbs energy of vacancy formation of fcc Ni. *Physical Review B*, 2018, vol. 97, p. 214106. DOI: 10.1103/physrevb.97.214106.
10. Lazurenko D.V., Dovzhenko G.D., Lozanov V.V., Petrov I.Y., Ogneva T.S., Emurlaev K.I., Bataev I.A. Stabilization of  $Ti_3Al_{11}$  at room temperature in ternary Ti–Al–Me (Me = Au, Pd, Mn, Pt) systems. *Journal of Alloys and Compounds*, 2023, vol. 944, p. 169244. DOI: 10.1016/j.jallcom.2023.169244.
11. Freysoldt C., Grabowski B., Hickel T., Neugebauer J., Kresse G., Janotti A., Van de Walle C.G. First-principles calculations for point defects in solids. *Reviews of Modern Physics*, 2014, vol. 86, iss. 1, pp. 253–305. DOI: 10.1103/revmodphys.86.253.
12. Zhang X., Grabowski B., Hickel T., Neugebauer J. Calculating free energies of point defects from ab initio. *Computational Materials Science*, 2018, vol. 148, pp. 249–259. DOI: 10.1016/j.commatsci.2018.
13. Giustino F. *Materials modelling using density functional theory: properties and predictions*. Oxford University Press, 2014. 286 p.
14. Kohn W., Sham L.J. Self-consistent equations including exchange and correlation effects. *Physical Review*, 1965, vol. 140, iss. 4A, pp. A1133–A1138. DOI: 10.1103/PhysRev.140.A1133.
15. Perdew J.P., Chevary J.A., Vosko S.H., Jackson K.A., Pederson M., Singh D.J., Fiolhais C. Atoms, molecules, solids, and surfaces: Applications of the generalized gradient approximation for exchange and correlation. *Physical Review B*, 1992, vol. 46, iss. 11, pp. 6671–6687. DOI: 10.1103/PhysRevB.46.6671.



16. Moll N., Bockstedte M., Fuchs M., Pehlke E., Scheffler M. Application of generalized gradient approximations: The diamond- $\beta$ -tin phase transition in Si and Ge. *Physical Review B*, 1995, vol. 52, iss. 4, pp. 2550–2556. DOI: 10.1103/PhysRevB.52.2550.
17. Nandi P.K., Valsakumar M.C., Chandra Sh., Sahu H.K., Sundar C.S. Efficacy of surface error corrections to density functional theory calculations of vacancy formation energy in transition metals. *Journal of Physics: Condensed Matter*, 2010, vol. 22, p. 345501. DOI: 10.1088/0953-8984/22/34/345501.
18. Delczeg L., Delczeg-Czirjak E.K., Johansson B., Vitos L. Density functional study of vacancies and surfaces in metals. *Journal of Physics: Condensed Matter*, 2011, vol. 23, p. 045006. DOI: 10.1088/0953-8984/23/4/045006.
19. Mortensen J.J., Hansen L.B., Jacobsen K.W. Real-space grid implementation of the projector augmented wave method. *Physical Review B*, 2005, vol. 71, iss. 3, p. 035109. DOI: 10.1103/PhysRevB.71.035109.
20. Enkovaara J., Rostgaard C., Mortensen J.J., et al. Electronic structure calculations with GPAW: a real-space implementation of the projector augmented-wave method. *Journal of Physics: Condensed Matter*, 2010, vol. 22, p. 243202. DOI: 10.1088/0953-8984/22/25/253202.
21. Enkovaara J., Rostgaard C., Mortensen J.J., et al. The atomic simulation environment – A Python library for working with atoms. *Journal of Physics: Condensed Matter*, 2017, vol. 29, iss. 27, p. 273002. DOI: 10.1088/1361-648X/aa680e.
22. Perdew J.P., Burke K., Ernzerhof M. Generalized gradient approximation made simple. *Physical Review Letters*, 1996, vol. 77, iss. 18, pp. 3865–3868. DOI: 10.1103/PhysRevLett.77.3865.
23. Patra B., Jana S., Constantin L.A., Samal P. Relevance of the Pauli kinetic energy density for semilocal functionals. *Physical Review B*, 2019, vol. 100, p. 155140. DOI: 10.1103/PhysRevB.100.155140.
24. Jana S., Behera S.K., Smiga S., Constantin L.A., Samal P. Improving the applicability of the Pauli kinetic energy density based semilocal functional for solids. *New Journal of Physics*, 2021, vol. 23, p. 063007. DOI: 10.1088/1367-2630/abfd4d.
25. Marzari N., Vanderbilt D., De Vita A., Payne M.C. Thermal contraction and disordering of the Al(110) surface. *Physical Review Letters*, 1999, vol. 82, iss. 16, pp. 3296–3299. DOI: 10.1103/PhysRevLett.82.3296.
26. Emery A.A., Wolverton C. High-throughput DFT calculations of formation energy, stability and oxygen vacancy formation energy of ABO<sub>3</sub> perovskites. *Scientific Data*, 2017, vol. 4, p. 170153. DOI: 10.1038/sdata.2017.153.
27. Hayashiuchi Y., Hagihara T., Okada T. A new interpretation of proportionality between vacancy formation energy and melting point. *Physica B+C*, 1982, vol. 115, iss. 1, pp. 67–71. DOI: 10.1016/0378-4363(82)90056-0.
28. Franklin A.D. Statistical thermodynamics of point defects in crystals. *Point Defects in Solids*. Boston, MA, Springer, 1972, p. 1–101. DOI: 10.1007/978-1-4684-2970-1\_1.
29. Doyama M., Koehler J.S. The relation between the formation energy of a vacancy and the nearest neighbor interactions in pure metals and liquid metals. *Acta Metallurgica*, 1976, vol. 24, iss. 9, pp. 871–879. DOI: 10.1016/0001-6160(76)90055-9.
30. Mattsson T.R., Mattsson A.E. Calculating the vacancy formation energy in metals: Pt, Pd, and Mo. *Physical Review B*, 2002, vol. 66, p. 214110. DOI: 10.1103/PhysRevB.66.214110.



## Detailed information about the parameters used in the computations

Table 1

 Details about metals used for *DFT* computations

Metal	Lattice type	Space group	Lattice parameters, Å		
			<i>a</i>	<i>b</i>	<i>c</i>
<i>Al</i>	<i>FCC</i>	225	4.0509		
<i>Ni</i>			3.5240		
<i>Cu</i>			3.6149		
<i>Rh</i>			3.8000		
<i>Pd</i>			3.8889		
<i>Ag</i>			3.8889		
<i>Ir</i>			3.8390		
<i>Pt</i>			3.9230		
<i>Au</i>			4.0773		
<i>Pb</i>			4.9500		
<i>Co</i>			3.4200		
<i>Li</i>	<i>BCC</i>	229	3.5100		
<i>Na</i>			4.2830		
<i>K</i>			5.3100		
<i>V</i>			3.0235		
<i>Cr</i>			2.8848		
<i>Fe</i>			2.8620		
<i>Rb</i>			5.6600		
<i>Nb</i>			3.3030		
<i>Mo</i>			3.1463		
<i>Ta</i>			3.3110		
<i>W</i>			3.1648		
<i>Be</i>	<i>HCP</i>	194	2.2860	3.5840	
<i>Zr</i>			3.2340	5.1480	
<i>Mg</i>			3.2092	5.2099	
<i>Sc</i>			3.3130	5.2760	
<i>Zn</i>			2.6575	4.9340	
<i>Y</i>			3.6435	5.7272	
<i>Ru</i>			2.7040	4.4000	
<i>Cd</i>			2.9790	5.6140	
<i>Hf</i>			3.1930	5.0520	
<i>Os</i>			2.7350	4.3200	
<i>Ti</i>			2.9400	4.6800	
<i>Co</i>	2.5071	4.0686			
<i>Re</i>	2.7600	4.4000			

Table 2

## Parameters for calculating the energy of bulk and vacancy supercells

Functional	Lattice type	$N$	$k$	$E_{PW}$	$MV$	$n$	$n_v$
<i>PBE</i>	<i>FCC</i>	$3 \times 3 \times 3$	$3 \times 3 \times 3$	500	0.2	108	107
	<i>BCC</i>					54	53
	<i>HCP</i>					108	107
<i>MGGAC</i>	<i>FCC</i>					108	107
	<i>BCC</i>					54	53
	<i>HCP</i>					108	107
<i>rMGGAC</i>	<i>FCC</i>					108	107
	<i>BCC</i>					54	53
	<i>HCP</i>					108	107

Note:  $E_{PW}$  – kinetic energy cutoff that determines the number of plane waves, eV;  $MV$  – the magnitude of the temperature broadening in the Marzari-Vanderbilt distribution, eV;  $n$  и  $n_v$  – the number of atoms in an ideal supercell and a supercell with a single vacancy. For all computations, periodic boundary conditions were set.

## Appendix B

## Values of vacancy formation energies in various elements

Table 3

Values of vacancy formation energies (eV) calculated in this work using the correlation-exchange functionals *PBE*, *MGGAC*, *MetaGGA*, along with the data from [8] (calculated values) and [7] (results of *PAS*)

No.	Metal	Lattice	<i>PBE</i>	<i>MGGAC</i>	<i>rMGGAC</i>	<i>LDA</i> [8]	<i>PBE</i> [8]	<i>PW91</i> [8]	<i>PAS</i> [7]
1	<i>Be</i>	<i>HCP</i>	0.96	1.65	1.75	–	–	–	–
2	<i>Mg</i>		0.85	0.96	1.07	0.8	0.77	0.72	–
3	<i>Sc</i>		2.01	2.4	2.51	1.97	1.86	1.8	–
4	<i>Zn</i>		0.41	0.68	0.76	0.5	0.42	0.49	–
5	<i>Y</i>		1.92	2.28	2.37	1.91	1.87	1.82	–
6	<i>Ru</i>		2.84	3.48	3.62	3.03	2.71	2.62	–
7	<i>Cd</i>		0.28	0.66	0.66	–	–	–	–
8	<i>Hf</i>		2.29	3.18	–	2.17	2.24	2.16	–
9	<i>Os</i>		3.04	3.8	–	3.35	3.08	3.02	–
10	<i>Ti</i>		2.23	2.87	2.99	2.08	2.08	1.99	–
11	<i>Co</i>		2.04	2.39	2.56	2.22	1.96	1.9	–
12	<i>Re</i>		3.24	3.86	–	3.65	3.4	3.26	–
13	<i>Zr</i>		2.19	2.82	2.95	–	–	–	–
14	<i>Li</i>	<i>BCC</i>	0.64	0.61	0.67	–	–	–	–
15	<i>Na</i>		0.43	0.48	–	0.34	0.33	0.31	–
16	<i>K</i>		0.37	0.41	0.44	0.33	0.3	0.29	0.34
17	<i>V</i>		2.98	3.49	3.76	–	2.27	2.2	2.07
18	<i>Cr</i>		3.05	3.93	4.1	2.85	2.77	2.65	2.0
19	<i>Fe</i>		1.86	2.58	2.71	2.3	2.2	2.14	–
20	<i>Rb</i>		0.32	0.37	0.4	–	–	–	–
21	<i>Nb</i>		3.0	3.49	3.71	3.01	2.77	2.71	2.65

End of the tab.3

No.	Metal	Lattice	<i>PBE</i>	<i>MGGAC</i>	<i>rMGGAC</i>	<i>LDA</i> [8]	<i>PBE</i> [8]	<i>PW91</i> [8]	<i>PAS</i> [7]
22	<i>Mo</i>		2.81	3.5	3.67	2.87	2.74	2.56	3.0
23	<i>Cs</i>		0.31	0.32	–	–	–	–	–
24	<i>Ta</i>		3.43	4.12	–	2.99	2.82	2.74	–
25	<i>W</i>		3.29	3.79	–	3.48	3.31	3.18	4.0
26	<i>Al</i>	<i>FCC</i>	0.74	0.7	0.96	0.71	0.65	0.56	0.66
27	<i>Ni</i>		1.51	2.09	2.19	1.68	1.46	1.89	–
28	<i>Cu</i>		1.04	1.77	1.8	1.29	1.09	1.05	1.28
29	<i>Rh</i>		1.64	2.22	2.31	2.02	1.74	1.66	–
30	<i>Pd</i>		1.06	1.74	1.75	1.48	1.21	1.18	1.85
31	<i>Ag</i>		0.03	0.77	0.77	1.05	0.78	0.77	1.11
32	<i>Ir</i>		1.57	2.52	–	1.89	1.62	1.57	1.79
33	<i>Pt</i>		0.67	1.46	–	0.99	0.74	0.72	1.32
34	<i>Au</i>		0.17	1.18	–	0.66	0.41	0.39	0.89
35	<i>Co</i>		1.75	2.58	2.66	2.1	1.8	1.76	1.34
36	<i>Pb</i>		–	0.81	–	–	–	–	–

## Conflicts of Interest

The authors declare no conflict of interest.

© 2023 The Authors. Published by Novosibirsk State Technical University. This is an open access article under the CC BY license (<http://creativecommons.org/licenses/by/4.0>).